Smart Health 28 (2023) 100387

Contents lists available at ScienceDirect

Smart Health

journal homepage: www.elsevier.com/locate/smhl

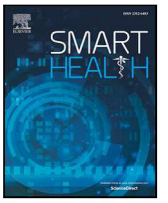

Respiratory biofeedback using acoustic sensing with smartphones

Azhar Chara [a,1], Tianya Zhao [b,1], Xuyu Wang [b,*], Shiwen Mao [c]

[a] Department of Computer Science, California State University, Sacramento, CA 95819, USA
[b] Knight Foundation School of Computing and Information Sciences, Florida International University, Miami, FL 33199, USA
[c] Department of Electrical and Computer Engineering, Auburn University, Auburn, AL 36849, USA

ARTICLE INFO

Keywords:
Biofeedback
Breath monitoring
Acoustic sensing
Smart health

ABSTRACT

Respiratory monitoring is a long-term tracking activity, which can be used to detect breathing abnormalities in patients with chronic diseases and also to manage psychological stress. However, sophisticated and expensive medical equipment is not suitable and convenient for long-term breathing monitoring. Therefore, an affordable contactless sensing system needs to be developed for long-term patient monitoring. In this paper, we propose a new contactless respiration monitoring system using acoustic sensing with smartphones. We design several algorithms to find the relationship between chest movements and breath signals. Beyond breathing rate monitoring, our system can also provide detailed respiration patterns, including inhalation and exhalation time, and apnea time, which can be used for real-time respiratory biofeedback during meditation. Our extensive experimental results show that the developed system can track real-time respiration, thus enabling accurate respiration patterns monitoring.

1. Introduction

The development of ubiquitous sensing technologies has led to the emergence of smart Internet of Things (IoT) devices that monitor and react to our daily activities (Adib et al., 2015). As health issues are becoming increasingly important, the need for health monitoring is expanding. In addition to using specialized but expensive instruments to monitor vital signals in hospitals, there is a growing demand for long-term self-monitoring at home by portable or wireless devices.

Among the various vital signs, the respiratory signal contains significant information that can effectively reflect the state of health. For instance, obstructive sleep apnea (OSA) is a chronic disease that increases cardiovascular morbidity and mortality risk (Norman & Loredo, 2008). Therefore, long-term sleep apnea monitoring is crucial to track OSA status and reduce the risk of cardiovascular disease. Heart rate variability (HRV) is a recognized surrogate for cardiac and mental health, reflecting the balance between the sympathetic and parasympathetic activity of the autonomic nervous system. By controlling the inhalation-to-exhalation (I:E) ratio, the HRV could be increased (Bae et al., 2021; Lin et al., 2014). Moreover, breathing exercises are helpful with respiratory disorders such as Asthma and chronic obstructive pulmonary disease (Holland et al., 2012; Holloway & Ram, 2004). Therefore, a system that can monitor and give feedback on respiratory information in real time is critical.

A variety of approaches have been deployed for detecting and monitoring respiration. Classic wearable devices, including smartwatches (Hao et al., 2017) and sensors attached to t-shirts (Mitchell et al., 2010), are widely used to monitor breathing. As a relatively mature technology, some commercial products already use wearable devices to obtain breathing patterns. For instance, Spire Health (2018) employs a passive health tag to detect patient health by monitoring breathing features such as

* Corresponding author.
E-mail addresses: azharchara@csus.edu (A. Chara), tzhao010@fiu.edu (T. Zhao), xuywang@fiu.edu (X. Wang), smao@ieee.org (S. Mao).
[1] Co-first Authors.

https://doi.org/10.1016/j.smhl.2023.100387
Received 15 March 2023; Accepted 15 March 2023
Available online 21 March 2023

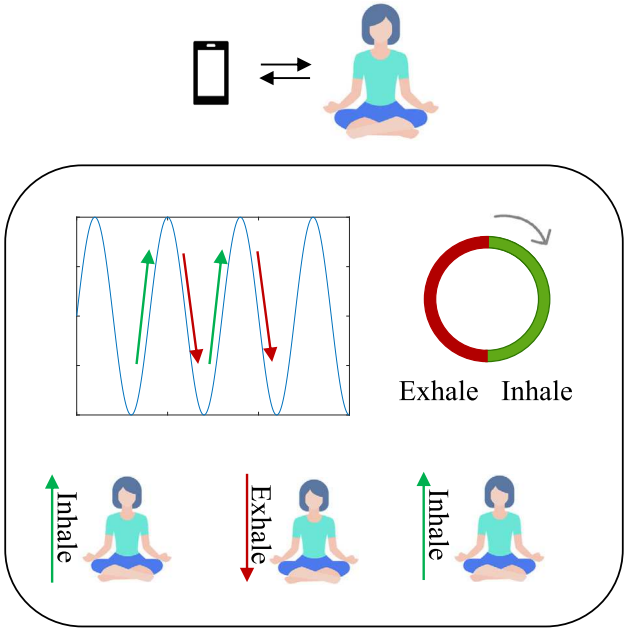

Fig. 1. Contactless respiratory biofeedback during meditation with acoustic sensing.

inhalation-to-exhalation ratio, breathing depth, and rate. However, long-term detection of respiration patterns and apnea with any wearable device is uncomfortable and inconvenient. Therefore, contactless activity monitoring is gaining great interest in academia and industry. Moreover, non-invasive long-term monitoring is essential for patients with chronic diseases. Existing works widely use wireless radio signals to monitor breathing activity, including sensor-based (Kroutil et al., 2016; Wang, Zhang, et al., 2019), radar-based (Vinci et al., 2013), and WiFi-based techniques (Wang et al., 2017a). However, relatively expensive hardware and complex device pairs (e.g., the WiFi-based methods need two smart devices) limit its applications.

Considering smartphone is a ubiquitous IoT device with built-in acoustic front-ends, this paper proposes a frequency-modulated continuous-wave (FMCW) acoustic sensing system based on only one smartphone. The system is accomplished by converting the smartphone into a sonar device (i.e., built-in speakers and microphones) that emits inaudible frequency-modulated sound waves and receives reflections from chest/abdomen movements (see Fig. 1). Although the FMCW method can easily detect respiration with acoustic devices, there are several challenges in our system. First, the time difference between transmitting and receiving signals fluctuates with time may result in incorrect estimation of distances. Second, it is crucial to distinguish between reflective signals from breathing actions and those from different environmental factors. As a result of the multipath effect, small periodic components generated by respiration may be easily overwhelmed by powerful static components (Mercuri et al., 2021). To address these issues, we propose two approaches: First, we eliminate the starting time difference by using the received signal without reflections (i.e., self-interference). Second, weak periodic respiration components can be identified by applying auto-correlation and Hilbert transform.

Ultimately, the proposed system successfully detects the breathing rate, respiration peak, apnea, inhalation time, and exhalation time in different scenarios. Our results show that the breathing median error is less than 0.15 BPM in various experiment environments.

The main contributions of this paper are summarized as follows:

- We propose an FMCW with an acoustic sensing system for respiration monitoring that can reach sub-centimeter range precision only through a smartphone. Correlation-based detection is used to determine the propagation time of audio signals using high-resolution samples. We also apply the Hilbert transform to envelope the correlation and use peak detection with prominence to better detect respiration patterns.
- We develop the system, which can effectively detect detailed respiration information, including breathing rate, breath pattern, inhalation and exhalation time, and apnea. All the information can be further used for monitoring health conditions or respiratory biofeedback during meditation.
- We conduct several experiments and demonstrate the effectiveness of the system. Specifically, we verify that our system can effectively monitor breath against various detection distances, breathing rates, apnea situations, and body movements.

In the rest of the paper, Section 2 reviews related work. Then, we describe the system model in Section 3. The experiment setup and the performance evaluation are in Section 4. We discuss limitations and future work in Section 5. Lastly, Section 6 summarizes this paper.

2. Related work

There are many works on respiration monitoring. Although contact-based methods (e.g., wearing a device) can be used for vital sign monitoring, they are not convenient while sleeping or applied for elders or baby monitoring. In this paper, we survey contactless respiratory monitoring works, which are classified into two main categories including customized device-based and commodity device-based.

2.1. Customized device-based methods

In order to detect human breathing, several customized devices are developed recently. Arlotto et al. (2014) measure the frequency variation generated by the velocity difference between the exhaled airflow and the surrounding environment based on a low-power ultrasonic active source and transducer. Boccanfuso and O'Kane (2012) monitor respiratory events by capturing changes in the sub-nasal skin surface temperature using a high-precision, single-point infrared sensor. Jian et al. (2014) apply an ultra-wideband (UWB) radar system with proper signal-processing algorithms to detect respiration and the system is able to detect tiny movements with ± 0.5 mm. Kiuru et al. (2016) present a 24 GHz FMCW radar system that uses changes in the received radar signals' statistical properties (i.e., amplitude and phase) to detect respiration. Rehman et al. (2021) deploy a universal software radio peripheral (USRP) model 2922 and omnidirectional antennas to construct the system, thus capturing the channel state information (CSI). WiBreath is a whole-home respiration rate sensing system that leverages a single transmitter–receiver pair (two Ettus USRP N210 devices) to monitor a person's respiration at a home scale (Ravichandran et al., 2015).

The primary concept is to track the changes produced by breathing. Except for the infrared sensor method, which monitors skin temperature changes due to breathing, most works detect chest movement. Even though these systems are accurate, they often require expensive devices such as transmitters, receivers, and specialized radio front-ends. Therefore, they are less suitable for widespread use in home monitoring scenarios due to the high price and complexity of the devices compared to commercial radios.

2.2. Commodity device-based methods

Methods based on RF signals: First, commodity WiFi devices are used for vital sign monitoring. Ubibreathe (Abdelnasser et al., 2015) extracts a person's breathing rate by measuring the WiFi received signal strength (RSS). CardioFi (Khamis et al., 2018) applies an enhanced sub-carrier selection mechanism to monitor heart rate through COTS WiFi hardware. Wital (Gu et al., 2021) exploits the relationship between the energy ratio of LOS/NLOS signals and the ability to monitor vital signs in real time. Liu et al. (2014) monitor breathing and heart rate by leveraging the amplitudes of WiFi CSI when the person is sleeping. PhaseBeat (Wang et al., 2017a, 2020) and Tensorbeat (Wang et al., 2017b) exploit WiFi CSI phase difference data to track single and multiple persons' vital signs, respectively. Wang et al. (2016) use the Fresnel model to investigate radio propagation in indoor scenarios and detect respiration patterns by analyzing the relation between chest movements and received WiFi signal amplitudes. Khamis et al. (2020) leverage the relationship between the changes in the CSI and breathing states to develop a respiratory biofeedback system based on WiFi. Second, off-the-shelf radar devices are exploited. For example, deep learning UWB radar systems are also proposed for robust vital sign monitoring, which can mitigate movement interference and environments changes (Chen et al., 2021; Xie et al., 2022; Zhang et al., 2022; Zheng et al., 2021).

Methods based on Audio: Wang et al. (2018) propose a C-FMCW-based respiration detection system using commodity audio devices. In this study, we utilize the default microphone and speaker of a smartphone, offering a more convenient approach. ApneaApp (Nandakumar et al., 2015) is a smartphone application that detects sleeping apnea events with FMCW. However, the limited sweeping band constrains the range resolution; hence, it is used to detect apnea events rather than more detailed respiration patterns. Hao et al. (2013) propose iSleep to monitor an individual's sleep quality by detecting body movement, cough, and snoring. BeepBeep (Peng et al., 2007) detects the roundtrip duration of the sound signal between two smartphones, but it needs to estimate the two devices' range first. RunBuddy (Hao et al., 2015) uses Bluetooth headphones to track a runner's breathing pattern and recommend an appropriate running pace. The headset may be acceptable for runners but may disturb sleeping users. BreathListener (Xu et al., 2019) uses energy spectrum density (ESD) of acoustic signals to capture breathing information in driving environments and deploys generative adversarial network (GAN) to generate breathing waveforms from the Hilbert spectrum of extracted respiration patterns. BreathJunior (Wang, Sunshine, & Gollakota, 2019) tracks motions and respiration by emitting multiple FMCW signals with random phases. LoEar (Wang et al., 2022) transmits orthogonal frequency-division multiplexing (OFDM) modulated acoustic signals and demodulates to obtain channel frequency response (CRF), and then detects dynamic reflections from vital signs.

The main distinction between our work and related acoustic sensing systems is that we can solely rely on a smartphone to monitor relatively extensive respiration patterns, including breathing rate, inhalation and exhalation time, and apnea. We have not only simplified the respiratory monitoring equipment but also ensured the validity of the results simultaneously.

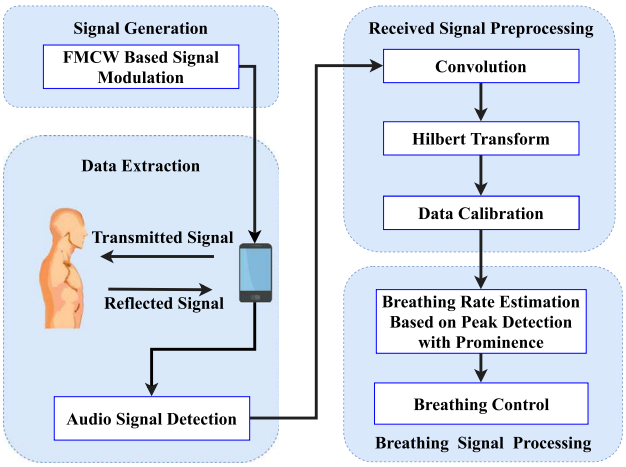

Fig. 2. System architecture for acoustic-based respiration monitoring.

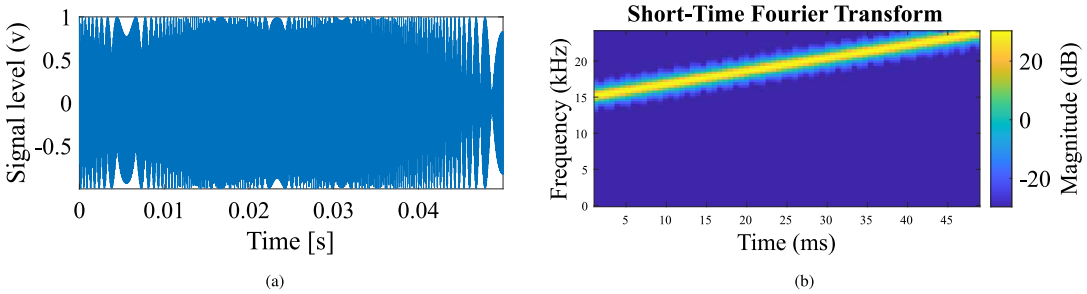

Fig. 3. Waveforms and spectrograms of the transmitted signals.

3. System model

3.1. System architecture

As shown in Fig. 2, our system consists of four main modules, including signal generation, data extraction, received signal preprocessing, and breathing signal processing. The signal generation module primarily implements the specification of an FMCW inaudible signal, which is created and modulated using MATLAB and the LibAS library (Tung et al., 2018) at the frequencies ranging from 15 kHz to 24 kHz. The LibAS library is exploited to connect a smartphone with a computer through a TCP/IP protocol. On the computer side, it is built to command and receive the acoustic signal sensed from the smartphone's microphone.

For the data extraction part, the smartphone's speaker transmits inaudible audio signals, and the microphone receives reflected signals from the chest and environments. However, received signals cannot directly reflect the respiratory pattern. Therefore, the received signal preprocessing part helps to analyze and extract the breathing signals. It consists of convolution, Hilbert transform, data calibration, and breath signal extraction. Convolution produces the correlation between transmitted and received signals. Then, the Hilbert transform takes out the envelope of convolution results. For data calibration, it detects the movements in the correlation and then removes high-frequency noises by a low-pass filter.

For the breathing signal processing part, we have a peak detection module for calculating the breathing beats per minute using respiratory signals. Specifically, the processed breath waveforms are obtained by detecting the actual peaks and removing the fake peaks through the prominence technique. We then further calculate the inhalation and exhalation time in a breath as our final result.

3.2. Signal generation and data extraction

The smartphone receives commands from a computer with the programmed code in MATLAB to transmit FMCW signals and receive reflected signals. The FMCW signal has the carrier frequency sweeping from 15 kHz to 24 kHz with a period of 0.05 s. The transmitted signal and its spectrogram are shown in Figs. 3(a) and 3(b), respectively. Besides, the sampling frequency is designated as 48 kHz. The transmitted signal can be formulated as follows.

$$s_{tx}(t) = A\cos(2\pi \int_o^t f(\tau)d\tau), \tag{1}$$

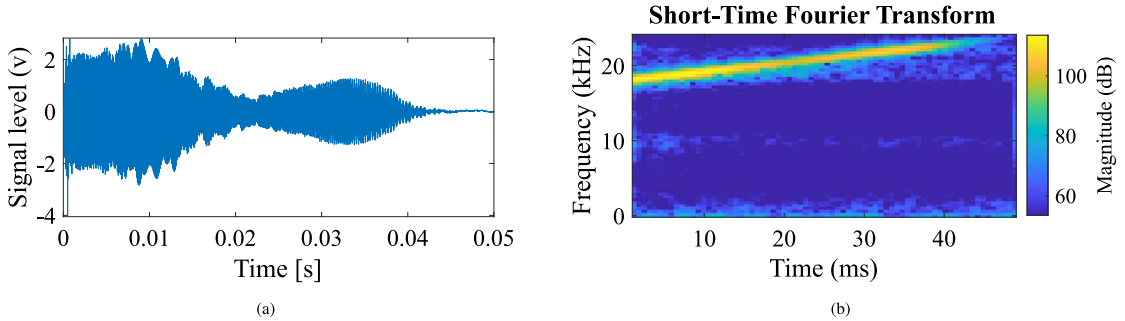

Fig. 4. Waveforms and spectrograms of the received signals.

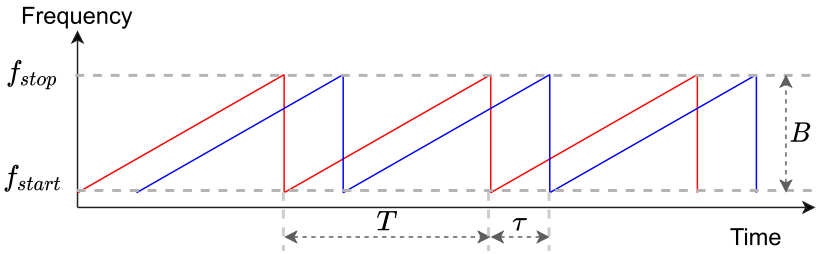

Fig. 5. Process of sweep frequency in FMCW signal.

where A is the amplitude (amplitude is considered to be 1 for the sake of simplicity), $f(\tau) = f_c + \frac{B\tau}{T}$ is the carrier frequency swiped in time, where f_c, B, and T denote initial carrier frequency, sweep bandwidth and sweep period, respectively. The process of the sweep frequency is shown in Fig. 5. The red line denotes the transmitted FMCW signal, and the blue line represents the received signal. The chirp signal with a linearly increasing frequency is transmitted to objects and reflected in a time delay τ.

The phase of the transmitted signal is calculated by integrating f_τ over time.

$$\phi(t) = 2\pi \int_o^t f(\tau)d\tau = 2\pi(f_c t + \frac{Bt^2}{2T}). \tag{2}$$

The transmitted signal is reflected by the target with the time delay τ. If the amplitude attenuation is ρ, the received signal at time t can be represented by,

$$s_{rx}(t) = \rho A \cos(2\pi(f_c(t-\tau) + \frac{B(t-\tau)^2}{2T})), \tag{3}$$

where the time delay τ is calculated by,

$$\tau = \frac{2(r+vt)}{c}, \tag{4}$$

where r denotes the distance between the transceiver and the target, v denotes the target's moving speed, and c denotes the speed of sound. The audio signals for breathing extraction are processed after a group of preamble signals are detected. Figs. 4(a) and 4(b) show the waveform and spectrograms of the received signals, respectively, in which we can see that the received signal is distorted versus the transmitted one due to the propagation environment of sound.

3.3. Received signal processing

As shown in Fig. 4(a), the receiver cannot detect the target through the received raw signal. Therefore, it is necessary to process the received signal for analysis. Due to the characteristics of FMCW signals, the receiver computes the correlation between the received signal with a copy of the transmitted signal for compressing. The correlation can be expressed by

$$R(\tau) = \int_0^T s_{rx}(t)s_{tx}(t-\tau)dt. \tag{5}$$

As shown in Fig. 6(a), the received signal is compressed after computing the correlation. However, it still needs to be clarified for analyzing respiration patterns. Therefore, we apply the *Hilbert transform* to find the envelope of the convolution results, which is a smooth curve outlining amplitudes. The procedure to determine the envelope is as follows,

$$\hat{x}(t) = H[x(t)] = \frac{1}{\pi}\int_{-\infty}^{\infty} \frac{x(\tau)}{t-\tau}d\tau, \tag{6}$$

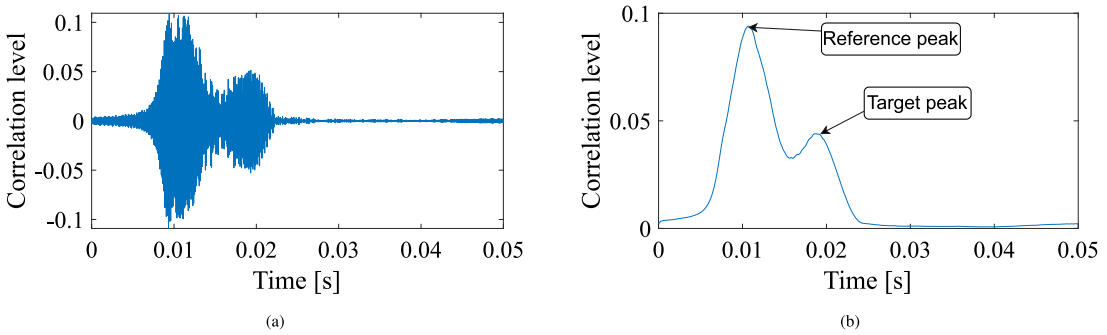

Fig. 6. Cross-correlation result between the received signal and the transmitted signal: (a) with the carrier frequency and (b) the envelope of the correlation.

where $\hat{x}(t)$ represents the result of the Hilbert transform of signal $x(t)$. By comparing with the convolution, it can be found that the expression of the Hilbert transform above fundamentally arises from convolving the original signal with $\frac{1}{\pi t}$.

$$\tilde{x}(t) = x(t) + j\hat{x}(t), \tag{7}$$

where we first construct the analytic signal $\tilde{x}(t)$, which is a complex-valued function with no negative frequency components. The real part of the analytic signal is the original signal, and the imaginary part is the signal after the Hilbert transform. Assume $x(t) = A(t)cos(2\pi f_c t)$, according to the properties of Hilbert transform, we have

$$\tilde{x}(t) = A(t)cos(2\pi f_c t) + jA(t)sin(2\pi f_c t) = A(t)e^{j2\pi f_c t}. \tag{8}$$

Therefore, the signal's envelope is the amplitude of the analytic signal, as shown in Fig. 6(b). The smooth envelope can be further calibrated and extracted to analyze breath waveforms.

3.4. Data calibration

As depicted in Fig. 6(b), two prominent peaks reveal that the received signals consist of an interference signal directly received by the microphone and a reflected signal transmitted from the speaker. For a transmitted signal (i.e., FMCW) with a modulation period T, the time delay within $T/2$ reflected from the target can be measured using the main peak of the cross-correlation (Wang et al., 2018). The cross-correlation values are used to estimate the chest's position because the reference peak is not from zero time. When a person breathes, the chest moves accordingly. Therefore, to better track the movement of the chest, the reference peak should be calibrated to the origin coordinates.

3.5. Breath signal processing

After the data calibration, we can extract the breathing signal by tracking the moving peaks corresponding to the chest movement. Because the signal is reflected not only by the chest movement but also by other parts of the body or surrounding objects, there are some unwanted peaks. If the system cannot distinguish fake peaks, it will affect its accuracy. For instance, the system will incorrectly estimate the breathing rate or the inspiration and expiration time because the peak of the breathing cycle cannot be accurately determined. The peak detection with prominence algorithm helps to eliminate the unwanted peaks and retain the peaks generated by chest movement.

Fig. 7 shows how to measure the prominence of a peak. First, we select one peak point, and then extend a horizontal line from the peak point to the left and right until the line intersects the signal or reaches the rightmost/leftmost end of the signal. In each of the two intervals, we locate the minimum (lowest) signal. It could be a valley or the signal may be ending at this moment. A comparison of the results using the conventional and peak detection with prominence algorithms will be presented later in Section 4.2.

3.6. LibAS library

In the proposed system, we adopt a LibAS tool, which is a cross-platform library that simplifies the creation of mobile acoustic sensor apps. It allows developers to quickly execute their ideas using a high-level Matlab script and test them across various platforms, including Android, iOS, Tizen, and Linux/Windows (KingFong, 2017). By concealing platform-specific characteristics, LibAS makes designing acoustic sensor apps easier. Developers do not need to know Objective-C/SWIFT or the CoreAudio framework's audio buffer management to construct acoustic sensing algorithms on an iPhone/Android. Instead, developers must select the detecting signals and the callback function to handle each signal's recurrence.

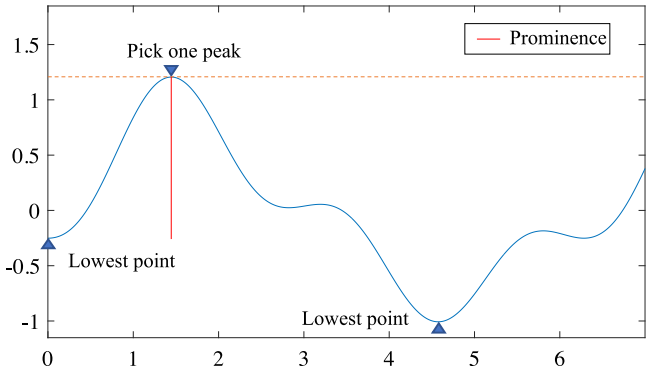

Fig. 7. Prominence calculation.

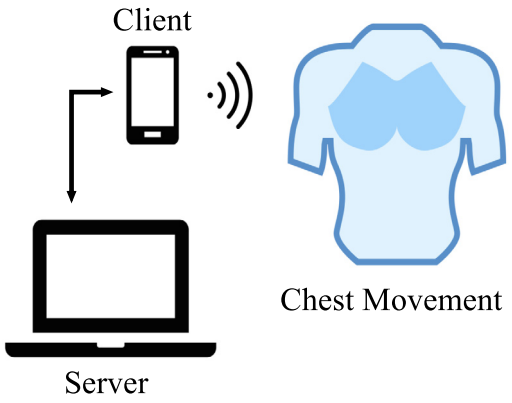

Fig. 8. Experimental setup.

4. Experiment results

In this section, we perform experiments to evaluate the proposed system. First, we describe our experiment settings. Afterward, we conduct comprehensive experiments to evaluate our system in different rooms with different subjects and three different body postures. We also evaluate the system's robustness at different sensing distances, breathing rates, and body movements.

4.1. Experiment settings

For the series of experiments, we utilize one laptop (Macbook Pro 2017 with Intel Core i7-8200 CPU, 16 GB RAM), and we connect our smartphone (OnePlus 6 or iPhone 6) to the laptop over the same WiFi network. As shown in Fig. 8, the laptop is a server, while the smartphone is a client. The client's speaker sends the FMCW signals continuously, and the client's microphone will receive the reflected signals and return them to the server controlled by MATLAB. During this process, the microphone receives the echo at a sampling rate of 48 kHz and transmits the inaudible audio signal to the server for data analysis and breathing detection. To prevent interference with other frequencies, the speaker broadcasts an FMCW signal with the parameters including the sample rate of 48 kHz, the period of one sensing repetition of sensing as 2400, the chirp length of 2400, the chirp starting frequency of 15 kHz, the chirp ending frequency of 24 kHz, the fading ration of 0.2, and the signal gain of 0.2. The smartphone's microphone receives the reflected signal at a frequency of 48 kHz and filters it with low-pass filters. The received signal from the abdomen is weak due to garment absorption and attenuation in the air. As a result, we leverage the smartphone near the subject's belly for active acoustic sensing for breathing signal monitoring.

4.2. Respiration rate estimation

In this paper, the breath period is defined by computing the average time interval between neighbor peaks. Then the breathing rate is estimated as follows:

$$Breathrate = \frac{60}{T_{breath}}, \tag{9}$$

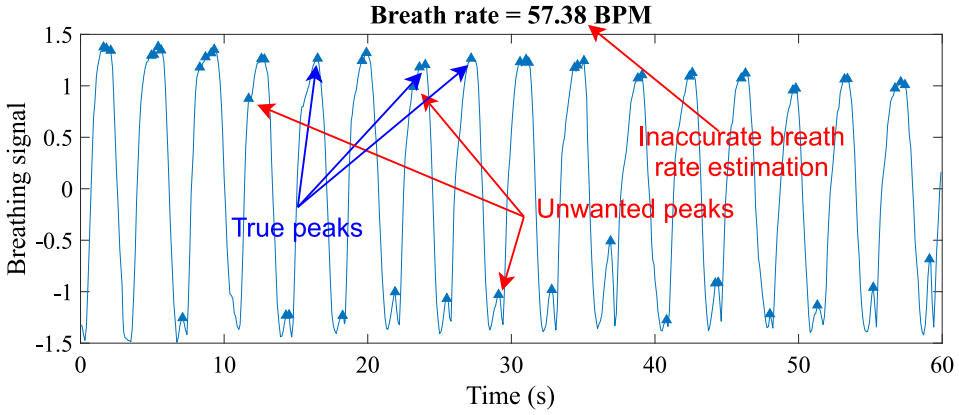

Fig. 9. Conventional peak detection algorithm for inaccurate breathing rate estimation.

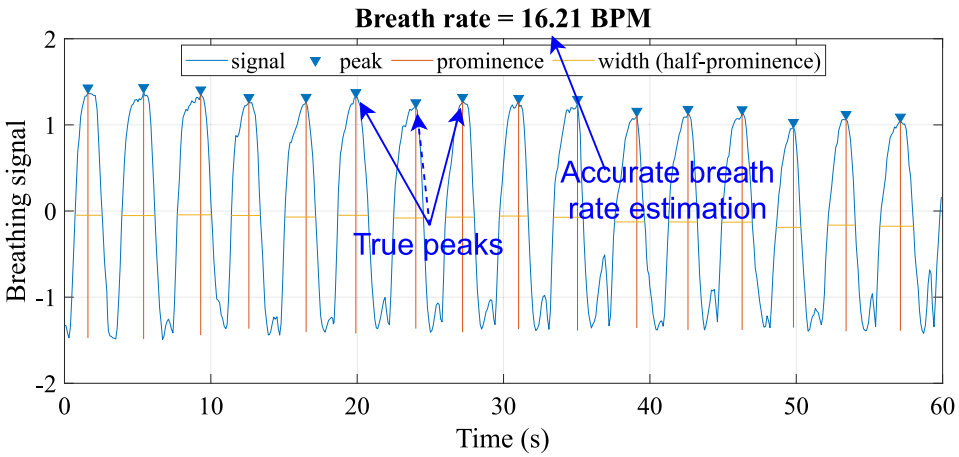

Fig. 10. Peaks detection with prominence. Peaks are correctly detected.

where T_{breath} is the breath period.

In some cases of unstable breathing or surrounding environment influence, the breath signal has unwanted peaks (or fake peaks). As shown in Fig. 9, the breathing rate is 57.38 BPM, while the actual rate is about 16 BPM. In a conventional peak detection algorithm, many fake peaks will be counted for estimating the breathing rate, thus leading to an erroneous result far from the ground truth.

As illustrated in Section 3.5, we use peak detection with prominence algorithm to filter fake peaks before calculating the breath period. For the breathing rate, inhalation, and exhalation time estimation, we need to detect two groups of peaks (i.e., top peaks and bottom peaks). As shown in Fig. 10, the breathing rate by using peak detection with prominence is 16.21 BPM, which is close to the ground truth. Therefore, peak detection with prominence is effective in extracting the true peaks in the breathing cycle.

4.3. Experiment results with/without smoothing

In real-world measurement, many moving objects in the surrounding environment affect the breathing signal quality and generate unwanted peaks, as shown in Fig. 11(a). Although we used a peak detection algorithm with prominence to eliminate the effect of false peaks on respiratory monitoring, some interfering peaks may still be present. The smoothing technique is used to remove excessively adjacent peaks, thus reducing the probability of misclassifying peaks. In our system, we leverage a smoothing technique with a window length of 20 samples to make the signal smoother. The improvement with the smoothing technique is provided in Fig. 11(b).

4.4. Experiment results with/without normalization

The received signal after the cross-correlation is always positive. Therefore, the generated breath signal is positive by tracking the mean value of the target peak. In order to highlight the top peaks and bottom peaks, we use the normalization technique to

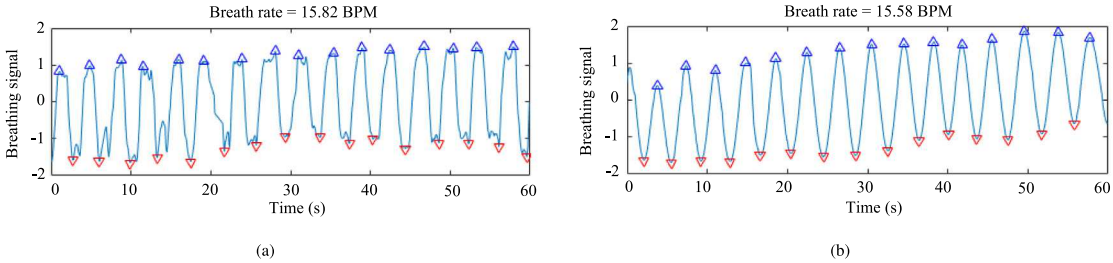

(a) (b)

Fig. 11. Breathing signal (a) without and (b) with the smoothing technique.

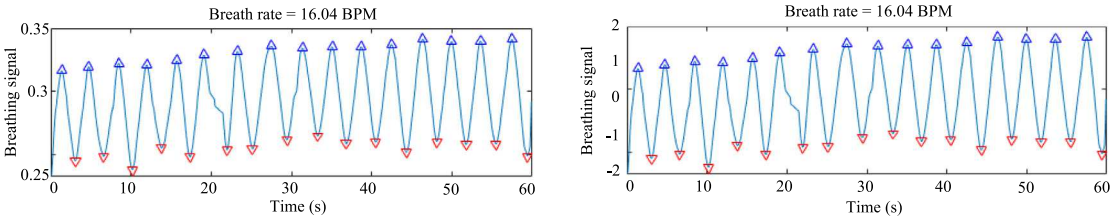

(a) (b)

Fig. 12. Breath signal (a) without and (b) with normalization.

translate the breath signal to a zero-mean value. After the normalization, the amplitude of the breathing waveform roughly ranges from −2 to 2, which can distinguish peaks and the respiration process. The normalization is expressed by,

$$x_o = \frac{x_i - \mu}{\sigma}, \tag{10}$$

where x_i denotes the input value, μ and σ are the mean and standard deviation value of x_i, respectively, x_o is the output corresponding to x_i. The comparison between the breath signal without and with the normalization is shown in Fig. 12.

4.5. Experiment results with different distances

The distance between the smartphone and the abdomen affects the breathing signal quality because the distance is directly related to the strength of the received signal. However, the distance does not have to be close or too far because of resolution and ambiguity issues. In this subsection, we measure the breathing signal with different distances, such as 10 cm, 20 cm, 30 cm, and 40 cm, and there is no obstacle between the smartphone and the body. The program needs to calibrate by manually setting the distance suitable to the actual distance. For the comparison, we breathe at a normal speed (12–16 BPM) for all distances. In the case of normal breathing, we can determine the stability of the breathing signal by judging the degree of the horizontal level of the peaks in one minute. Results in Fig. 13 show that the proposed method can successfully capture the breath signal with different distances. In all four cases, all peaks are monitored, and the respiration rate is correctly calculated. Interestingly, the distance of 40 cm achieves the most stable breathing signal, probably due to the unambiguous phase condition.

4.6. Experiment results with different breathing rates

This part evaluates the breath signal with different respiration rates, such as 7 BPM, 14 BPM, 20 BPM, and 37 BPM. As shown in Fig. 14, the proposed method can correctly measure the breath signal with different breathing rates. Specifically, the measured breath signal is more stable for a regular respiration rate of 14 BPM and less stable for a slower or faster breathing rate, probably due to the irregular movements of the abdomen during abnormal speed breathing. In the case of 7 BPM, there are some plateaus in the waveform. This is mainly because the abdomen will keep static for a while when the person breathes slowly (e.g., deep breathing). For the 37 BPM case, we can find some short breath cycles because exhaling is quickly followed by inhaling at a high BPM.

4.7. Experiment results with body movement

The main task of our system is to identify the respiration pattern. By using the auto-correlation method, we establish the periodicity of all distance sequences. We then choose the distance sequence corresponding to the major reflection path that best reflects respiration if all the distance sequences' periodicities are smaller than a certain threshold. Therefore, interference factors like body movements can be detected in this way. While the user's body posture changes, the result of the respiration recognition

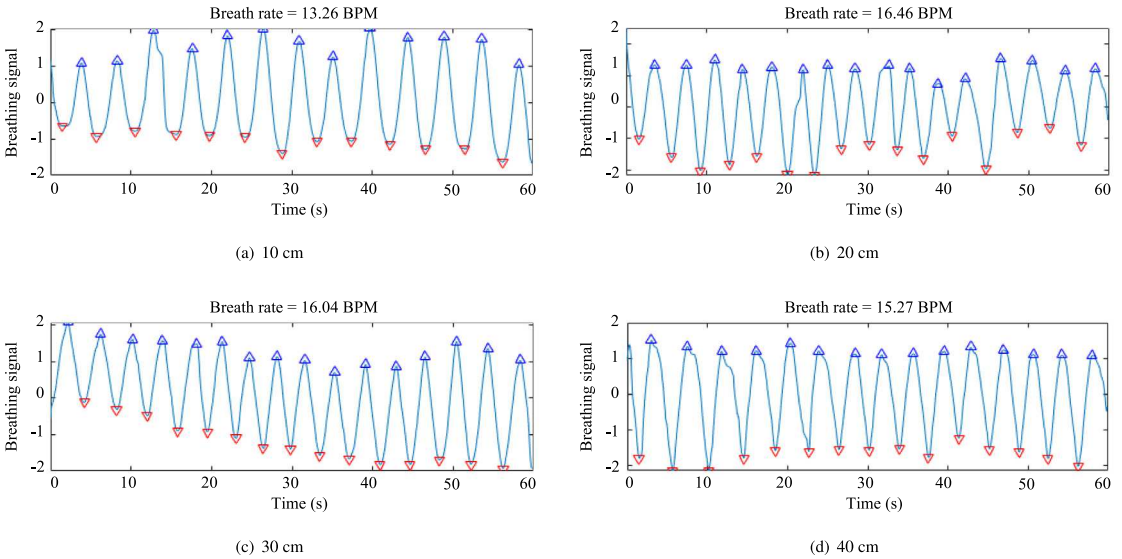

(a) 10 cm (b) 20 cm

(c) 30 cm (d) 40 cm

Fig. 13. Breath signals with different distances.

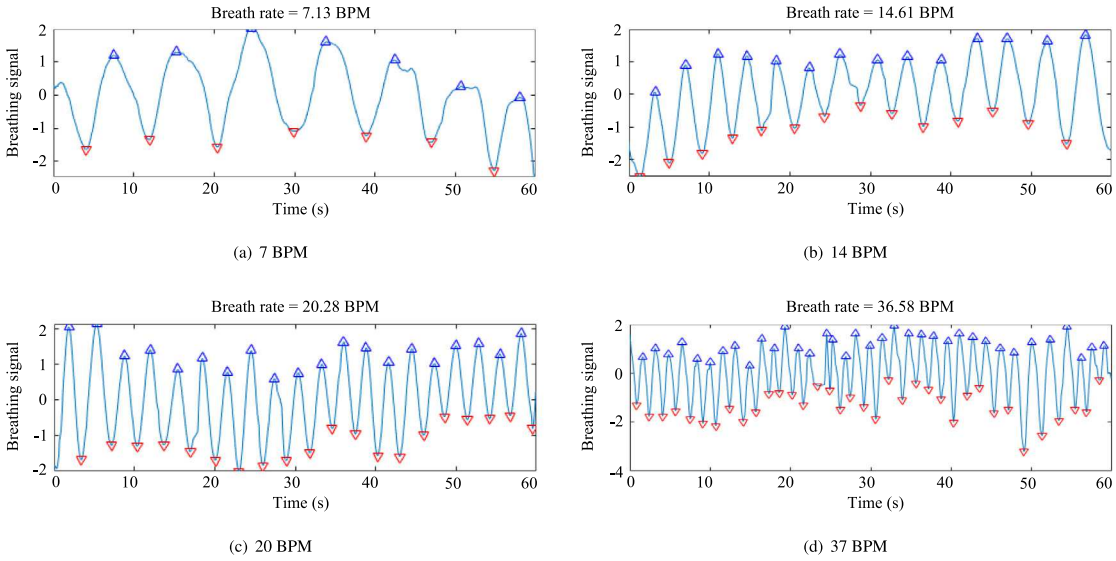

(a) 7 BPM (b) 14 BPM

(c) 20 BPM (d) 37 BPM

Fig. 14. Breath signal with different respiration rates.

is displayed in Fig. 15. The waveform is irregular in the body movement part, and the amplitude of one peak substantially exceeds that of the others. Moreover, there are more unwanted peaks than normal status.

Before the body moves, the system monitors the respiratory and shows waveform normally. The breath waveform is drastically irregular and cannot give reasonable peaks when the body moves. Because the system cannot effectively capture chest movements when the distance fluctuates, the system will stop recognizing breaths at this time. Once at least one distance sequence's frequency exceeds a threshold and the body stabilizes, the system will restore its ability and continue monitoring breathing to improve the system's accuracy.

4.8. Experiment results to detect apnea

This section detects two different types of apnea; one is inhalation stop, and the other is exhalation stop. The experiment is performed as follows. First, the person starts breathing normally at time 0, then stops breathing at a deep exhalation and keeps static. Then, this person restarts normal breathing at 16 s. Next, this person stops breathing at 40 s when inhales deeply. As shown

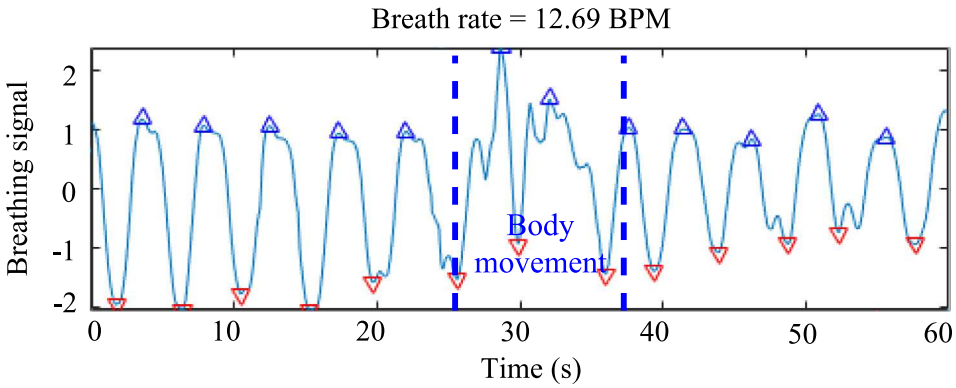

Fig. 15. Breath signal with body movement.

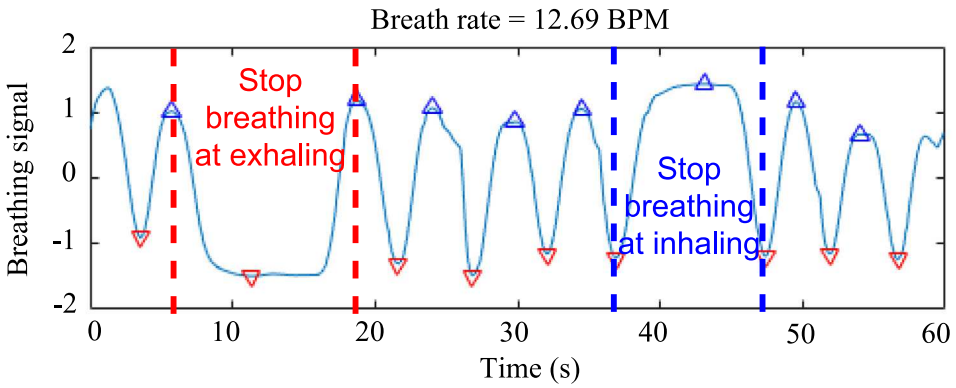

Fig. 16. Breath signal with stop breathing at inhaling and exhaling.

in Fig. 16, we observe that the system reacts correctly when the person stops and restarts breathing. All the regular peaks and apnea plateaus are displayed accordingly, and apnea does not interfere with the subsequent monitoring of normal breathing. The breathing rate has a slight deviation because the system calculates it by the average period.

4.9. Inhale and exhale time estimation

For the inhalation and exhalation time estimation, we need to detect the bottom peaks in addition to the group of top peaks. By changing the sign of breathing signal values, we can easily convert the bottom peaks to the top peaks. Then, we process the converted peaks in the same way as before for the top peaks. Afterward, the bottom peaks will be detected. After calculating the time difference between the top and bottom peaks, we can estimate inhalation and exhalation time, as shown in Fig. 17. It displays that the system can detect the specific inhalation and exhalation time and further calculate the I:E ratio. As we discussed before, we can adjust our breathing patterns to precisely control the I:E ratio to help improve many health problems, specifically for respiratory biofeedback during meditation.

5. Discussion

Although experimental results show that the proposed system can detect human breathing and be adapted to various real-world scenarios, including different sensing distances, changing breathing rates, simulated apnea, and body movements, the current implementation has the limitations as follows.

First, the microphone must be placed immediately in front of the abdomen to receive reflected acoustic waves. Wearing a heavy fabric or covering with a quilt and having a different prostrate can affect accuracy because the chest displacements may be too small to be detected at this point. Moreover, the robustness of the system may need further improvement because there may be some bias in the results of respiratory monitoring for people with different body sizes.

Second, this paper only aims to extract the breath information caused by the small chest and abdomen movements. We can explore breathing information more deeply. As we discussed before, the I:E ratio is a crucial indicator of health conditions. We can focus on improving the system's ability to detect the I:E ratio in more scenarios since we can already detect inhalation and

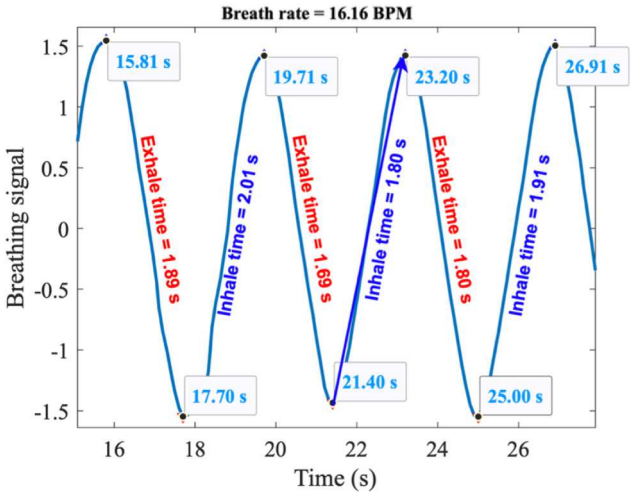

Fig. 17. Inhale and exhale time estimation.

exhalation time during a normal breath. Furthermore, mental health has become an increasing concern in recent years, and our system can also be designed to determine stress and mental state by detecting breathing patterns. Besides, other physiological data can also be exploited. For example, our system could theoretically extract heart rate without contact with the human body. Previous RF-based radar systems (Rong & Bliss, 2018) have shown that heart rate can be extracted from wireless signals with a gigahertz bandwidth due to its high range resolution. Therefore, if the sampling rate increases, we may detect small movements, such as finger gestures or mechanical vibrations. We will explore the phase of the FMCW signal for vital sign monitoring, and combine deep learning techniques to improve the system's robustness.

6. Conclusion

This paper presented a contactless respiratory biofeedback monitoring system by leveraging a smartphone's speaker and microphone. We first introduced the system architecture in detail, including signal generation, detection, preprocessing, and breathing signal processing. To solve specific practical issues in the FMCW-based acoustic sensing system, we incorporated some valid signal processing algorithms (e.g., Hilbert transform and peak detection with prominence). Then, we conducted extensive experiments in various settings, including different distances, breathing rates, and respiration patterns. The experimental results demonstrated that our system could accurately detect breathing rates and respiration patterns (e.g., inhalation and exhalation time) in various conditions.

Declaration of competing interest

The authors declare that they have no known competing financial interests or personal relationships that could have appeared to influence the work reported in this paper.

Data availability

Data will be made available on request.

Acknowledgments

This work is supported in part by the NSF, United States (CNS-2107190, CNS-2105416, CNS-2321763, and CNS-2107164).

References

Abdelnasser, H., Harras, K. A., & Youssef, M. (2015). Ubibreathe: A ubiquitous non-invasive wifi-based breathing estimator. http://dx.doi.org/10.1145/2746285.2755969, arXiv preprint arXiv:1505.02388.

Adib, F. M., Mao, H., Kabelac, Z., Katabi, D., & Miller, R. (2015). Smart homes that monitor breathing and heart rate. In *Proceedings of the 33rd annual ACM conference on human factors in computing systems*.

Arlotto, P., Grimaldi, M., Naeck, R., & Ginoux, J.-M. (2014). An ultrasonic contactless sensor for breathing monitoring. *Sensors*, *14*(8), 15371–15386. http://dx.doi.org/10.3390/s140815371, URL https://www.mdpi.com/1424-8220/14/8/15371.

Bae, D., Matthews, J. J., Chen, J. J., & Mah, L. (2021). Increased exhalation to inhalation ratio during breathing enhances high-frequency heart rate variability in healthy adults. *Psychophysiology*, *58*(11), Article e13905. http://dx.doi.org/10.1111/psyp.13905.

Boccanfuso, L., & O'Kane, J. M. (2012). Remote measurement of breathing rate in real time using a high precision, single-point infrared temperature sensor. In *2012 4th IEEE RAS & EMBS international conference on biomedical robotics and biomechatronics* (pp. 1704–1709). http://dx.doi.org/10.1109/BioRob.2012.6290703.

Chen, Z., Zheng, T., Cai, C., & Luo, J. (2021). MoVi-Fi: Motion-robust vital signs waveform recovery via deep interpreted RF sensing. In *Proceedings of the 27th annual international conference on mobile computing and networking* (pp. 392–405). http://dx.doi.org/10.1145/3447993.3483251.

Gu, Y., Zhang, X., Yan, H., Liu, Z., & Ji, Y. (2021). Real-time vital signs monitoring based on COTS WiFi devices. In *2021 IEEE international conference on bioinformatics and biomedicine* (pp. 1320–1324). IEEE, http://dx.doi.org/10.1109/BIBM52615.2021.9669403.

Hao, T., Bi, C., Xing, G., Chan, R., & Tu, L. (2017). MindfulWatch: A smartwatch-based system for real-time respiration monitoring during meditation. *Proceedings of ACM Interactive Mobile Wearable Ubiquitous Technology*, *1*, 57:1–57:19.

Hao, T., Xing, G., & Zhou, G. (2013). Isleep: Unobtrusive sleep quality monitoring using smartphones. In *Proceedings of the 11th ACM conference on embedded networked sensor systems* (pp. 1–14). http://dx.doi.org/10.1145/2517351.2517359.

Hao, T., Xing, G., & Zhou, G. (2015). RunBuddy: A smartphone system for running rhythm monitoring. In *Proceedings of the 2015 ACM international joint conference on pervasive and ubiquitous computing* (pp. 133–144). http://dx.doi.org/10.1145/2750858.2804293.

Holland, A. E., Hill, C. J., Jones, A. Y., & McDonald, C. F. (2012). Breathing exercises for chronic obstructive pulmonary disease. *Cochrane Database of Systematic Reviews*, (10), http://dx.doi.org/10.1002/14651858.CD008250.pub2.

Holloway, E. A., & Ram, F. S. (2004). Breathing exercises for asthma. *Cochrane Database of Systematic Reviews*, (1), http://dx.doi.org/10.1002/14651858.CD001277.pub2.

Jian, Q., Yang, J., Yu, Y., Björkholm, P., & McKelvey, T. (2014). Detection of breathing and heartbeat by using a simple UWB radar system. In *The 8th European conference on antennas and propagation* (pp. 3078–3081). http://dx.doi.org/10.1109/EuCAP.2014.6902477.

Khamis, A., Chou, C. T., Kusy, B., & Hu, W. (2018). CardioFi: Enabling heart rate monitoring on unmodified COTS WiFi devices. In *Proceedings of the 15th EAI international conference on mobile and ubiquitous systems: Computing, networking and services* (pp. 97–106). http://dx.doi.org/10.1145/3286978.3287003.

Khamis, A., Kusy, B., Chou, C. T., & Hu, W. (2020). WiRelax: Towards real-time respiratory biofeedback during meditation using WiFi. *Ad Hoc Networks*, *107*, Article 102226. http://dx.doi.org/10.1016/j.adhoc.2020.102226.

KingFong (2017). Libas DevApp. URL https://appadvice.com/app/libas-devapp/1292387567.

Kiuru, T., Metso, M., Jardak, S., Pursula, P., Häkli, J., Hirvonen, M., & Sepponen, R. (2016). Movement and respiration detection using statistical properties of the FMCW radar signal. In *2016 Global symposium on millimeter waves (GSMM) & ESA workshop on millimetre-wave technology and applications* (pp. 1–4). http://dx.doi.org/10.1109/GSMM.2016.7500331.

Kroutil, A., Husák, M., & Sio, R. (2016). Acoustic method for respiratory monitoring. In *2016 11th International conference on advanced semiconductor devices & microsystems* (pp. 117–120). http://dx.doi.org/10.1109/ASDAM.2016.7805909.

Lin, I.-M., Tai, L., & Fan, S.-Y. (2014). Breathing at a rate of 5.5 breaths per minute with equal inhalation-to-exhalation ratio increases heart rate variability. *International Journal of Psychophysiology*, *91*(3), 206–211. http://dx.doi.org/10.1016/j.ijpsycho.2013.12.006.

Liu, X., Cao, J., Tang, S., & Wen, J. (2014). Wi-Sleep: Contactless sleep monitoring via WiFi signals. In *2014 IEEE real-time systems symposium* (pp. 346–355). http://dx.doi.org/10.1109/RTSS.2014.30.

Mercuri, M., Lu, Y., Polito, S., Wieringa, F., Liu, Y.-H., van der Veen, A.-J., Van Hoof, C., & Torfs, T. (2021). Enabling robust radar-based localization and vital signs monitoring in multipath propagation environments. *IEEE Transactions on Biomedical Engineering*, *68*(11), 3228–3240. http://dx.doi.org/10.1109/TBME.2021.3066876.

Mitchell, E., Coyle, S., O'Connor, N. E., Diamond, D., & Ward, T. (2010). Breathing feedback system with wearable textile sensors. In *2010 International conference on body sensor networks* (pp. 56–61). http://dx.doi.org/10.1109/BSN.2010.31.

Nandakumar, R., Gollakota, S., & Watson, N. (2015). Contactless sleep apnea detection on smartphones. In *Proceedings of the 13th annual international conference on mobile systems, applications, and services* (pp. 45–57). http://dx.doi.org/10.1145/2742647.2742674.

Norman, D., & Loredo, J. S. (2008). Obstructive sleep apnea in older adults. *Clinics in Geriatric Medicine*, *24*(1), 151–165.

Peng, C., Shen, G., Zhang, Y., Li, Y., & Tan, K. (2007). Beepbeep: A high accuracy acoustic ranging system using cots mobile devices. In *Proceedings of the 5th international conference on embedded networked sensor systems* (pp. 1–14). http://dx.doi.org/10.1145/1322263.1322265.

Ravichandran, R., Saba, E., Chen, K.-Y., Goel, M., Gupta, S., & Patel, S. N. (2015). WiBreathe: Estimating respiration rate using wireless signals in natural settings in the home. In *2015 IEEE international conference on pervasive computing and communications* (pp. 131–139). IEEE, http://dx.doi.org/10.1109/PERCOM.2015.7146519.

Rehman, M., Shah, R. A., Khan, M. B., AbuAli, N. A., Shah, S. A., Yang, X., Alomainy, A., Imran, M. A., & Abbasi, Q. H. (2021). RF sensing based breathing patterns detection leveraging USRP devices. *Sensors*, *21*(11), http://dx.doi.org/10.3390/s21113855, URL https://www.mdpi.com/1424-8220/21/11/3855.

Rong, Y., & Bliss, D. W. (2018). Direct RF signal processing for heart-rate monitoring using UWB impulse radar. In *2018 52nd Asilomar conference on signals, systems, and computers* (pp. 1215–1219). http://dx.doi.org/10.1109/ACSSC.2018.8645559.

Spire Health (2018). Spire health: Home. URL https://www.spirehealth.com/.

Tung, Y.-C., Bui, D., & Shin, K. G. (2018). Cross-platform support for rapid development of mobile acoustic sensing applications. In *Proceedings of the 16th annual international conference on mobile systems, applications, and services* (pp. 455–467). http://dx.doi.org/10.1145/3210240.3210312.

Vinci, G., Lindner, S., Barbon, F., Mann, S., Hofmann, M., Duda, A., Weigel, R., & Koelpin, A. (2013). Six-port radar sensor for remote respiration rate and heartbeat vital-sign monitoring. *IEEE Transactions on Microwave Theory and Techniques*, *61*(5), 2093–2100. http://dx.doi.org/10.1109/TMTT.2013.2247055.

Wang, L., Li, W., Sun, K., Zhang, F., Gu, T., Xu, C., & Zhang, D. (2022). LoEar: Push the range limit of acoustic sensing for vital sign monitoring. *Proceedings of the ACM on Interactive, Mobile, Wearable and Ubiquitous Technologies*, *6*(3), 1–24. http://dx.doi.org/10.1145/3550293.

Wang, A., Sunshine, J. E., & Gollakota, S. (2019). Contactless infant monitoring using white noise. In *The 25th Annual international conference on mobile computing and networking* (pp. 1–16). http://dx.doi.org/10.1145/3300061.3345453.

Wang, X., Yang, C., & Mao, S. (2017a). PhaseBeat: Exploiting CSI phase data for vital sign monitoring with commodity WiFi devices. In *2017 IEEE 37th International conference on distributed computing systems* (pp. 1230–1239). http://dx.doi.org/10.1109/ICDCS.2017.206.

Wang, X., Yang, C., & Mao, S. (2017b). TensorBeat: Tensor decomposition for monitoring multiperson breathing beats with commodity WiFi. *ACM Transactions on Intelligent Systems and Technology*, *9*(1), 1–27. http://dx.doi.org/10.1145/3078855.

Wang, X., Yang, C., & Mao, S. (2020). On CSI-based vital sign monitoring using commodity WiFi. *ACM Transactions on Computing for Healthcare*, *1*(3), 1–27. http://dx.doi.org/10.1145/3377165.

Wang, H., Zhang, D., Ma, J., Wang, Y., Wang, Y., Wu, D., Gu, T., & Xie, B. (2016). Human respiration detection with commodity wifi devices: Do user location and body orientation matter? In *Proceedings of the 2016 ACM international joint conference on pervasive and ubiquitous computing* (pp. 25–36). http://dx.doi.org/10.1145/2971648.2971744.

Wang, T., Zhang, D., Wang, L., Zheng, Y., Gu, T., Dorizzi, B., & Zhou, X. (2019). Contactless respiration monitoring using ultrasound signal with off-the-shelf audio devices. *IEEE Internet of Things Journal*, *6*(2), 2959–2973. http://dx.doi.org/10.1109/JIOT.2018.2877607.

Wang, T., Zhang, D., Zheng, Y., Gu, T., Zhou, X., & Dorizzi, B. (2018). C-FMCW based contactless respiration detection using acoustic signal. *Proceedings of the ACM on Interactive, Mobile, Wearable and Ubiquitous Technologies*, *1*(4), 1–20. http://dx.doi.org/10.1145/3161188.

Xie, Z., Wang, H., Han, S., Schoenfeld, E., & Ye, F. (2022). DeepVS: A deep learning approach for RF-based vital signs sensing. In *Proceedings of the 13th ACM international conference on bioinformatics, computational biology and health informatics* (pp. 1–5). http://dx.doi.org/10.1145/3535508.3545554.

Xu, X., Yu, J., Chen, Y., Zhu, Y., Kong, L., & Li, M. (2019). Breathlistener: Fine-grained breathing monitoring in driving environments utilizing acoustic signals. In *Proceedings of the 17th annual international conference on mobile systems, applications, and services* (pp. 54–66). http://dx.doi.org/10.1145/3307334.3326074.

Zhang, S., Zheng, T., Chen, Z., & Luo, J. (2022). Can we obtain fine-grained heartbeat waveform via contact-free RF-sensing? In *IEEE INFOCOM 2022-IEEE conference on computer communications* (pp. 1759–1768). IEEE, http://dx.doi.org/10.1109/INFOCOM48880.2022.9796905.

Zheng, T., Chen, Z., Zhang, S., Cai, C., & Luo, J. (2021). MoRe-Fi: Motion-robust and fine-grained respiration monitoring via deep-learning UWB radar. In *Proceedings of the 19th ACM conference on embedded networked sensor systems* (pp. 111–124). http://dx.doi.org/10.1145/3485730.3485932.